Detecting Nitrous Oxide from Silage Gas Using Fourier Transform Infrared Spectroscopy and Linefit Program

Achide Samson Achide
Department of Basic Sciences,
College of Agriculture,
P.M.B 33 Lafia Nasarawa State, Nigeria.
*Email of the corresponding Author: achidesamson@gmail.com/gistwitachide@yahoo.com

Abstract
Fourier Transform InfraRed (FTIR) spectroscopy is an excellent analytical technique needed for measuring greenhouse gases like the Nitrogen dioxide (N_2O) rapidly in the atmosphere resulting from agricultural practices. Measurement of greenhouse gases using FTIR, have led to many important advances in our understanding of the atmosphere. In this study, N_2O gases produced during the early phase of silage processing from corn ensiling using FTIR Spectroscopy at $1cm^{-1}$ spectral resolution derived from LINEFIT program were measured from a laboratory bucket silo. Excess gases produced in the bucket silos were collected and filled into a 5litre Tedlar bag during the first week after ensiling. Absorption peak fingerprints of N_2O were identified in the FTIR spectra of the silage gas using both standard N_2O gas spectra and simulated spectra from the Infrared spectral database. N_2O concentrations retrieved from three spectral regions of the 5–ppm spectrum were averaged 4.98 ± 0.09 *ppm. These confirms N_2O accurately retrieved from FTIR spectra using LINEFIT program. Laboratory bucket silos do provide a realistic model system for lab-scale silage gas measurements. It holds potential for lab-scale evaluations of silage fermentations as well as the possibility of investigating the effects of different initial packing densities and use of different wrapping materials.*

Keyswords: *Greenhouse Gas, Silage Gas, Nitrous Oxide, Fourier transform Spectroscopy and LINEFIT Program.*

1.0 Introduction

Greenhouse gases and the potential for global climate change are receiving increased attention by countries and in international forums. Many of the options for responding to concerns about global climate change have very significant implications for the production and use of various forms of energy. While there is public concern over greenhouse gases, global warming and global change, there is also widespread recognition of uncertainties concerning other air quality issues emitted from human activities or natural systems (sources) and sinks.

Greenhouse gas emission from anthropogenic sources since Industrial revolution, estimates 37% of the total greenhouse gas emission for non – carbon dioxide (CO_2) gases (Forester *et al.*, 2007). While many factors continue to influence greenhouse gases, scientists have determined that human activities have become a dominant force, and are responsible for most of the global warming observed over the past 50 years. The balance between sources (emissions of the gas from human activities and natural systems) and sinks (the removal of the gas from the atmosphere by

conversion to a different chemical compound IPCC, 2007b) can determine the atmospheric concentrations of greenhouse gases.

Greenhouse gases (GHG) are those gaseous constituents of the atmosphere, both natural and anthropogenic, that absorb and emit radiation at specific wavelengths within the spectrum of thermal infrared radiation emitted by the Earth's surface, the atmosphere itself, and by clouds (IPCC, 2007a). This process is the fundamental cause of the greenhouse effect and fig. 1 shows the schematic view of the components of climatic system, processes and interactions.

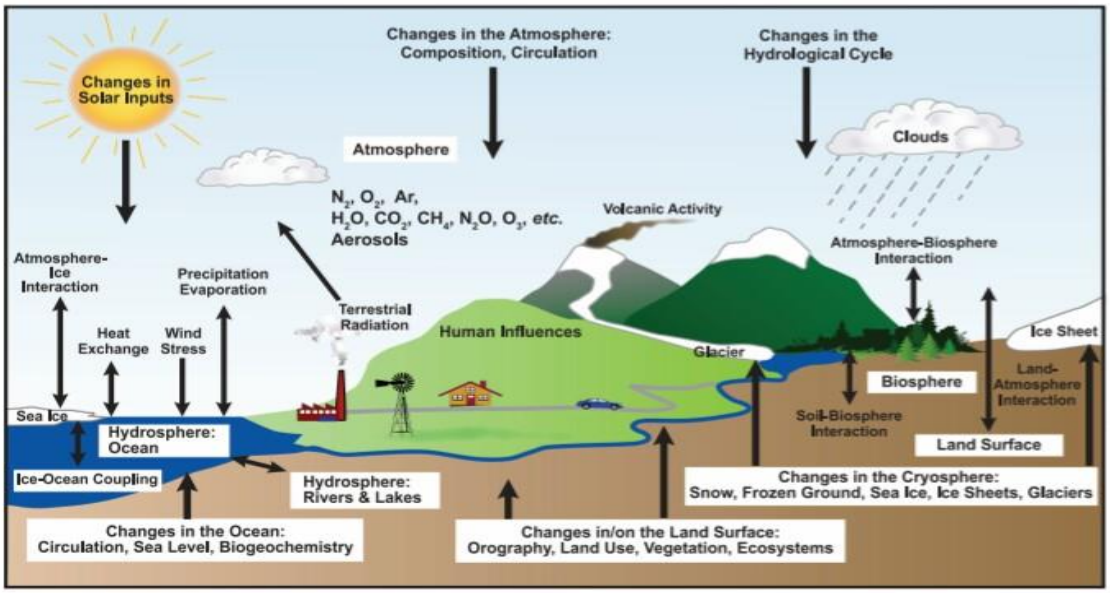

Figure 1: Schematic view of the components of the climate system, their processes and interactions.

Some primary greenhouse gases (GHG) in the atmosphere that are entirely manmade are halocarbons and other chlorine and bromine-containing substances referred to as the Montreal Protocol gases. The Kyoto Protocol regulates emission of the following gases: Carbon dioxide (CO_2), Nitrous Oxide (N_2O), Methane (CH_4), Sulphur Hexafluoride (SF_6), Hydrofluorocarbons (HFCs) and Perfluorocarbons (PFCs), with equivalence to CO_2 based on their global warming potential (GWP). GWP used in the Kyoto protocol are shown in Intergovernmental Policy on Climate Change (IPCC) assessments as stated by Forester *et al.*, 2007 and Ramaswamy *et al.*, 2001. It is been estimated that if greenhouse gas emissions continue at their present rate, Earth's surface temperature could exceed historical values as early as 2047, with potentially harmful effects on ecosystems, biodiversity and the livelihoods of people worldwide (Mora, 2013). Recent estimates also suggest that at current emission rates the Earth could pass a threshold of 2°C global warming, which the United Nations' IPCC designated as the upper limit to avoid "dangerous" global warming, by 2036 (Mann, 2014).

Today, various techniques contribute to the effort of monitoring the atmosphere's gaseous composition. Most practical multi – gas mitigation strategies require metrics to relate the climate effects of CO_2 to the climate effects of other greenhouse gases (IPCC, 2009). In view of making the climate impact of different GHG comparable, they are normally converted to CO_2 equivalents.

CO_2 is thereby the reference gas against which other gases are measured and has a global warming potential of 1. The global warming potential represents how much a certain mass of a gas contributes to global warming compared to the same mass of CO_2. It is based on the different times "gases remain in the atmosphere and their relative effectiveness in absorbing outgoing thermal infrared radiation" (IPCC, 2007b).

Silage is an important preservation technique, used worldwide to provide nutritious and palatable animal feed months after harvest (Weinberg and Ashbell, 2003). It is estimated that 200 million tons of dry matter (DM) are ensiled worldwide annually (Weinberg and Ashbell, 2003; Bacenetti and Fusi, 2015). A significant fraction of the nutritive value of silage is lost due to biological oxidation and the biochemical production relying on lactic acid anaerobic fermentation.

Nitrous oxide (N_2O) is an important long-lived greenhouse gas (GHG) also emitted during silage processes with a global warming potential (GWP) of 265 compared to carbon dioxide (CO_2) (GWP = 1) and methane (CH_4) (GWP = 28) (Myhre, *et al*., 2013). Unlike CO_2 and CH_4, the inventory of N_2O emissions remains largely uncertain because some of the N_2O emission sources have not yet been systematically quantified, such as those from agricultural sources, landfills, and wastewater treatment systems. Various gas emissions from silage, except for N_2O have been investigated by various laboratory and field experiments (Reid *et al.*,1984; Hafner et *al.*, 2013; Hafner *et al.*, 2014). The N_2O emissions from silage corn cropland have been estimated worldwide by Linn and Doran 1984; Van Groenigen *et al.*, 2004; Liu *et al.*, 2014. Wang and Burries (1960) monitored nitrogenous gases produced by silage in both field and laboratory silos using a mass spectrometer. They reported a maximum N_2O concentration of 4.35% in the farm silo gas at about 54 hours after ensiling. This was possible because N_2O and CO_2 both have a mass of 44, with N_2O signals obtained by differentiating them from CO_2 peaks in the mass spectra. Little information has been available on N_2O produced by silage since the Wang and Burries measurements. This was because silage gases produced during the early phase of ensiling were studied mostly for toxicity (Reid *et al.*,1984).

Since insufficient attention has been given and scarce data available on N_2O as an important GHG gas emitted during the silage making process, the study was undertaken to analyse N_2O gases produced during the early phase of silage processing from complex mixture of corn ensiling using Fourier Transform Infrared (FTIR) Spectroscopy derived from LINEFIT program.

2. Mathematical Background

2.1. Data Acquisition from Fourier Transform Infrared (FTIR) Spectrometer

According to Herres (1984), Infrared light emitted by a source is directed to a beam splitter that travels to a fixed mirror through a distance L at a total path length of 2L. The moving back and forth of the reflecting mirror of the interferometer around L by a distance X, gives a total path length of the beam as

$$2 * (L + X) \quad \text{---------- 1}$$

The beam leaving the interferometer is focused on the detector, which is the measure of intensity $I(X)$ of the combined IR beams. These partial waves interfere constructively yielding maximum detector signal if their optical retardation is an exact multiple of the wavelength (λ) given as

$$2 \times X = n \times \lambda \ (\mathrm{n} = 0,1,2, \dots \dots \dots \dots \dots) \quad \text{---------- 2}$$

Bergland (1969) stated that the complete dependence of $I(X)$ on x is given by a cosine function

$$I(X) = S(v) * Cos(2\pi \cdot v \cdot x) \quad \text{---------- 3}$$

Where wave number $(v) = {}^{1}/_{\lambda}$ and

$S(v)$ is the intensity of the monochromatic line located at wave number v.

The accuracy of the sample spacing Δx between two zero crossings is solely determined by the precision of the laser wavelength itself. The spacing Δv in the spectrum is inversely proportional to Δx. This wave number calibration of high precision give rise to the cones advantage.

2.2. Fourier Transformation

According to Bell (1972), data acquisition from Infrared spectrometer yields the digitalized interferogram $I(X)$, which is converted into a spectrum by means of a mathematical operation called Fourier transformation. If the interferogram is sampled and consist of N discrete equidistant points

$$S(k \cdot \Delta v) = \sum_{n=0}^{N-1} I(n \cdot \Delta x)\, exp\left(\frac{i2\pi nk}{N}\right) \quad \text{---------- 4}$$

Where the continuous variables x, v have been replaced by $n \cdot \Delta x$ and $k \cdot \Delta x$ respectively.

The spacing Δv in the spectrum is related to Δx by

$$\Delta v = {}^{1}/_{(N.\Delta x)} \quad \text{---------- 5}$$

With the resulting new function $S(k.\Delta v)$ called the Fourier coefficients, one can easily reconstruct the interferogram $I(n \cdot \Delta x)$ by combining all cosines and sines multiplied by their Fourier coefficients $S(k.\Delta v)$ and dividing the whole sum by their number of points N given as

$$I(n \cdot \Delta x) = \left({}^{1}/_{N}\right) \sum_{n=0}^{N-1} S(k \cdot \Delta v)\, exp\left(-i2\pi \cdot \frac{nk}{N}\right) \quad \text{-------- 6}$$

2.3 Spectrum Calculation

According to Harris (1978), Fourier transformation may produce artifacts such as Aliasing. From Equ. 4, practical calculations for both n and k will run from 0 to $N-1$. This means, the Fourier transform of an N point interferogram yields only $\frac{N}{2}$ meaningful output points. If from Equ. 4 index k is substituted by $N-k$ using the identity

$$\begin{aligned} expi2nk &= (expi2\pi) ** k \\ &= 1 ** k \\ &= 1 \end{aligned} \quad \text{---------- 7}$$

With equ. 7 one obtains the mathematical description of mirror symmetry

$$S([N-k]) = S(-k) \quad \text{---------- 8}$$

Furthermore, equ. 4 is not only valid for indices k from 0 to $N-1$ but for all intergers including negative numbers, replacing k in equation 4 by $k + m.N$, one obtains,

$$S([k + m.N]) = S(k) \quad \text{---------- 9}$$

From equ. 9, it becomes clear that a unique spectrum can only be calculated if the spectrum does not overlap with its mirror – symmetrical replicate. Since no overlap will occur if the spectrum is zero above a maximum wave number v_{max} or if v_{max} is smaller than the Nyquist wavenumber v_f, then

$$v_{max} \leq v_f = \left({}^{N}/_{2}\right) \cdot \Delta v = {}^{1}/_{(2.\Delta x)} \text{ ---------- 10}$$

Mathematically, an interferogram $IL(x)$ as stated by Herres and Gronholz (1984) that is truncated at optical path difference $x = L$ can be obtained by multiplying an interferogram $Ii(x)$ of infinite extension by a 'boxcar' function $BX(x)$, which is zero for $x > L$ or $x \leq L$

$$IL(x) = Ii(x) \cdot BX(x) \text{ ---------- 11}$$

According to the convolution theorem of Fourier analysis, if $Si(v)$ and $bx(v)$ are the Fourier transform of $Ii(x)$ and $BX(x)$ respectively, then

$$Si(v) = \int_{-\infty}^{+\infty} exp(i2\pi vx) \cdot Ii(x)dx$$

$$bx(v) = \int_{-\infty}^{+\infty} exp(i2\pi vx) \cdot BX(x)dx$$

Seeking the relation for the Fourier transform $SL(v)$ of the truncated interferogram $IL(x)$ gives

$$SL(v) = \int_{-}^{+\infty} \exp(i2\pi vx) \cdot IL(x)dx$$

$$= \int_{-\infty}^{+\infty} \exp(i2\pi vx)\, Ii(x)BX(x)dx$$

$$= \int_{-\infty}^{+\infty} Si(k)b(x)(v-k)dk$$

$$= Si(v)\, O\, bx(v) \text{ ---------- 13}$$

According to Mertz (1967), a complex spectrum $C(v)$ can be represented by the sum

$$C(v) = R(v) + iI(v) \text{ ---------- 14}$$

of a purely real part $R(v)$ and a purely imaginary part $I(v)$ or equivalently, by the product

$$C(v) = S(v)\exp(i\emptyset(v)) \text{ ---------- 15}$$

of the true 'amplitude' spectrum $S(v)$ and the complex exponential $\exp(i\emptyset(v))$ containing the wave number dependent 'phase' $\emptyset(v)$.

To extract the amplitude of $S(v)$ from the complex output $C(v)$ of the Fourier transform, the square root of the power spectrum is calculated as

$$P(v) = C(v) \cdot C^*(v)$$

$$S(v) = [C(v) \cdot C^*(v)]^{1/2}$$

$$= [R^2(v) + I^2(v)]^{1/2} \text{ ---------- 16}$$

Or by multiplication of $C(v)$ by the inverse of the phase exponential and taking the real part of the result given as;

$$S(v) = Re[C(v)\exp(-i\emptyset\,(v))] \text{ ---------- 17}$$

From equ. 17 which is computed by interpolation from low resolution phase spectrum, the corrected real part $R'(v)$ which represents the final channel spectrum $S(v)$ is stored for further processing given as

$$R'(v) = R(v)\cos\big(\emptyset(v)\big) - I(v)\sin(\emptyset(v)) \text{ ---------- 18}$$

While the corrected imaginary part

$$I'(v) = R(v)\sin\big(\emptyset(v)\big) + I(v)\cos(\emptyset(v)) \text{ ---------- 19}$$

Originates from the antisymmetric contribution, which would have been zero if a double-sided interferogram had been used.

2.4. LINEFIT Program

LINEFIT is an instrumental line shape retrieval program and the knowledge of the instrument line shape (ILS), or the observed shape of a spectral line from a monochromatic input, is crucial in assessing instrument performance and avoiding unknown biases in retrievals. Two parameters in the LINEFIT algorithm (Hase *et al.,* 1999) are used to characterize the ILS in relation to an ideal instrument, namely the modulation efficiency (ME) and phase error (PE). The LINEFIT code is in wide use within the FTIR group of the Network for Detection of Atmospheric Composition Change (NDACC) and Total Carbon Column Observing Network (TCCON) (Wunch *et al.,* 2007) for the analysis of reference gas cell spectra recorded with high-resolution (Hase, 2012 and Hase *et al.*, 2013).

3. Sample Preparation in Laboratory Bucket Silos

Various types of laboratory silos for decades had been used to simulate the conditions of large-scale silos for different purposes (Neal and Becker, 1933; Johnson *et al.,* 2005). Procedures to make corn silage in laboratory bucket silos and collect gas samples from the bucket silos have already been described by Hafner *et al.*, 2014.

In this study, twelve kilograms of corn forage samples were manually compressed into an 18.9 litre bucket silos. Excess gases produced in the bucket silos were collected and filled into a 5litre Tedlar bag during the first week after ensiling.

The bag of the silage gas is then setup to be analyzed by the FTIR spectroscopy to investigate what compounds were present in the silage gas.

Since the properties of the silage gas samples produced in the bucket silos were similar to typical values (Hafner *et al.,* 2014), the gas sample collected should be representative of the complex mixture of the silage gas.

3.1. FTIR Instrumental Setup for Silage Gas Verification

The FTIR spectrometer was coupled with a long-path White Cell. Before switching the silage gas samples in the White Cell, the White Cell was flushed three times by alternatively evacuating the chamber down below 1hPa and filling it with pure nitrogen (N_2) to 1013hPa. The White Cell was operated at ambient pressure to prevent any contamination to gas samples due to possible leaks. Prior to switching of the silage gas samples in the White Cell, the air samples from the bucket silos is to be diluted by a factor of 3.2 in the White Cell.

When analyzing pure N_2 and standard N_2O gas samples, the White Cell were filled with either pure N_2 or standard N_2O gas to 1013hPa. In analyzing the silage gas, 5 litres of silage gas from a 5litre Tedlar bag plus 11 litres of high purity N_2 were added to the White Cell to bring the pressure up to 1013hPa into the White Cell. The optical path length of the White Cell was adjusted close to its maximum of 64 meters in order to maximize instrument sensitivity and therefore detect weak absorption signals. First, the FTIR spectrum of the high purity N_2 was recorded as background.

Then, the FTIR spectrum of the silage gas plus N_2 mixture was recorded. In order to confirm that N_2O absorptions were identified correctly, the FTIR spectrum of a 5-ppm standard N_2O gas were recorded.

4. Results

4.1. FTIR Spectra of the Silage Gas and Verification of N_2O Peaks

Significant N_2O absorption peaks were found in the FTIR spectra of the silage gas as shown in Fig. 2 in a spectra region of 1850.0 – 2850.0 cm^{-1} at 1cm^{-1} spectral resolution.

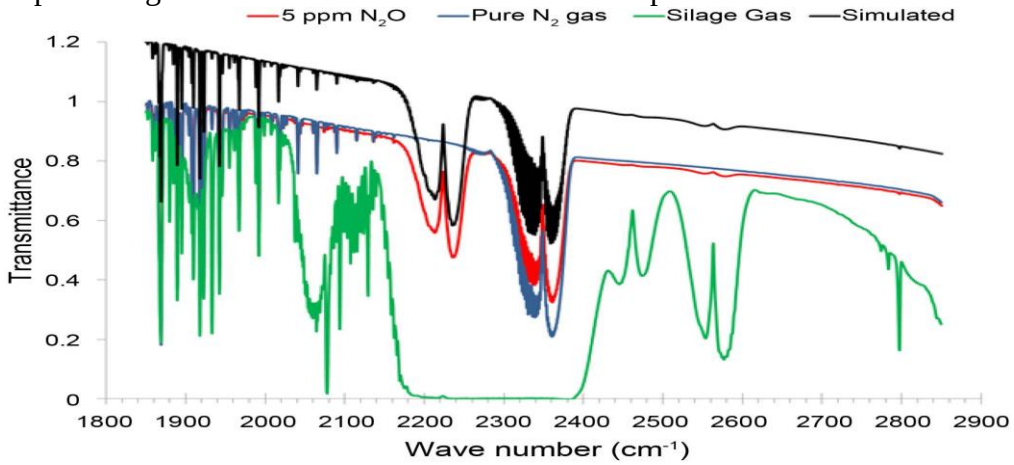

Figure 2. FTIR spectra of air samples from laboratory bucket silos in a spectra region of 1850.0 – 2850.0 cm^{-1} at 1cm^{-1} spectral resolution.

4.2. Selection of the Spectral Windows Using LINEFIT Program

A. The 5-ppm standard N_2O spectrum in Figure 2 showed that;

1. N_2O absorption at the fundamental and associated "hot bands" was not saturated between 2130.0 and 2270.0 cm^{-1}.
2. The absorption of CO_2 at the fundamental band located at 2349.0 cm^{-1} was not saturated either. Therefore, three spectral windows can be used to retrieve the 5-ppm N_2O spectrum:
   i) 2140.0 - 2285.0 cm^{-1}
   ii) 2130.0 - 2650.0 cm^{-1}
   iii) 2510.0 - 2615.0 cm^{-1}. Shown in Figure 3 – 5.

B. In the spectrum of the silage gas, two spectral windows were selected to retrieve the N_2O concentrations at;

i) 2140.0 – 2615.0 cm^{-1} and
ii) 2510.0 – 2615.0 cm^{-1}. Shown in Figure 6 and 7.

Also when fitting the spectral window at 2140 – 2615 cm^{-1}, a special technique in the LINEFIT program, called "de-weighting", was applied to the sub-window between 2300 and 2510 cm^{-1} because of the complexity of CO_2 absorptions in this region.

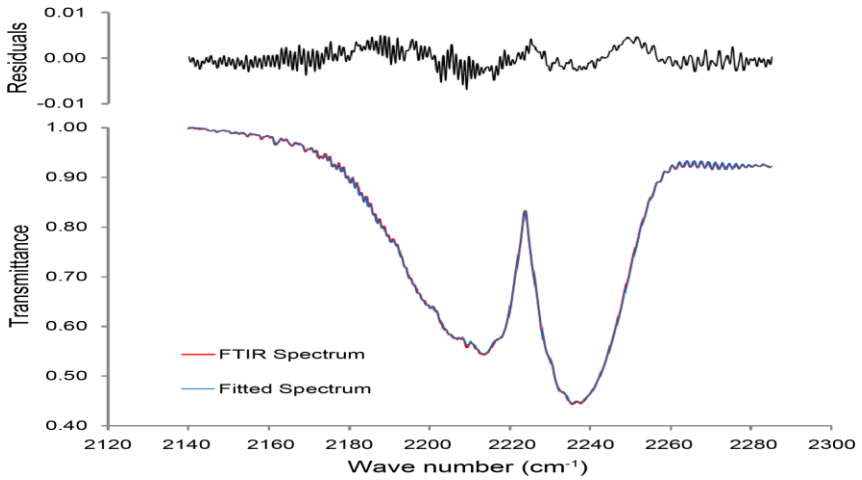

Figure 3. Retrieval of the 5-ppm N_2O spectrum at window 2140 – 2285 cm^{-1}.

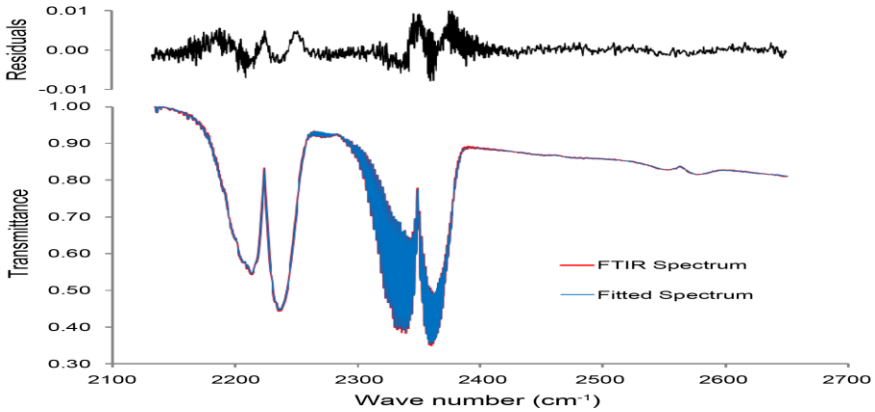

Figure 4. Retrieval of the 5-ppm N_2O spectrum window at 2130 – 2650 cm^{-1}

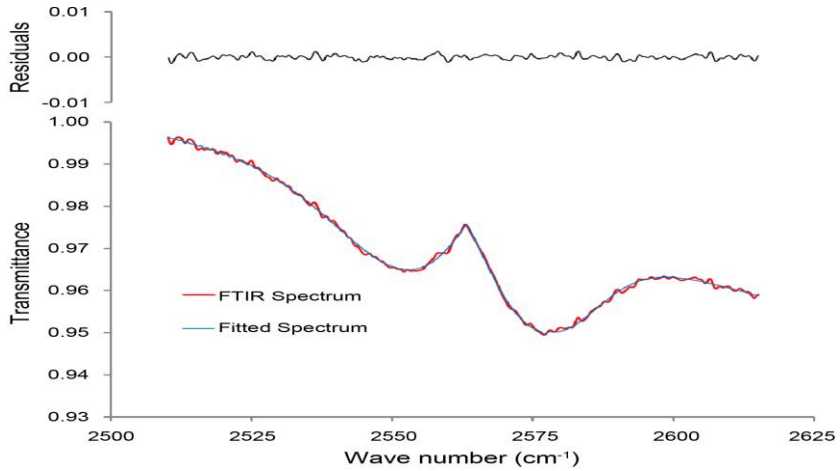

Figure 5. Retrieval of the 5-ppm N_2O spectrum window at 2510 – 2615 cm^{-1}

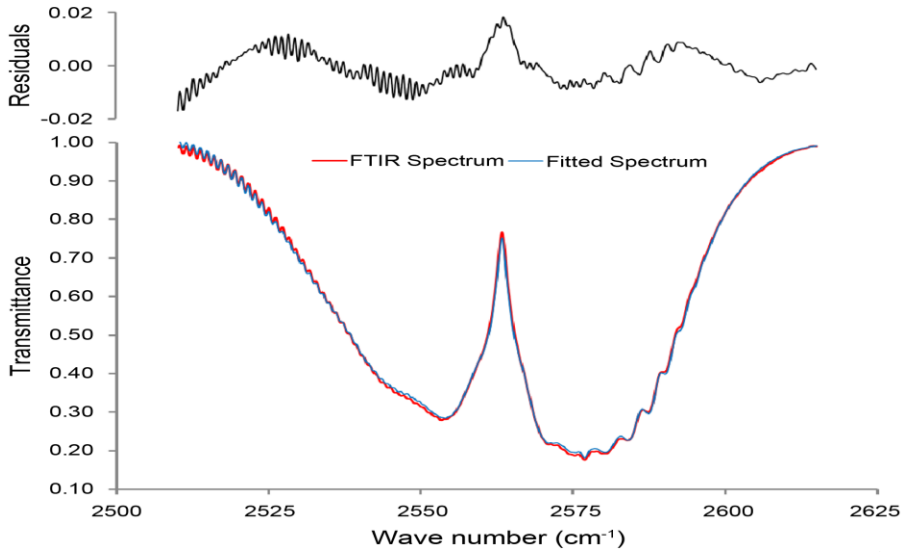

Figure 6. Retrieval of bucket silos samples spectrum window at 2510 – 2615 cm^{-1}

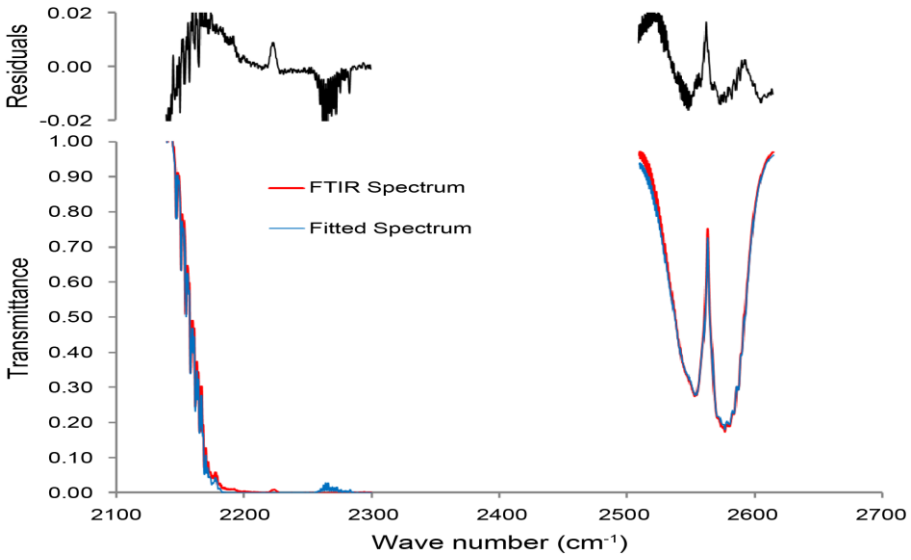

Figure 7. Retrieval of bucket silos samples spectrum at window 2140 – 2615 cm^{-1} with sub – window at 2300 – 2510 cm^{-1}

5. Discussion:

It can be seen from fig. 2 that the absorption of the silage gas in the region of 2130 – 2270 cm^{-1} was saturated while the absorption of the 5 –ppm N_2O in the same region was not, indicating that N_2O concentration in the silage gas were much higher than 5 – ppm. Also, the absorption of the silage gas in the region of 2400 – 2600 cm^{-1} were not saturated and by comparison, the absorption of the 5 – ppm N_2O gas in this region were weaker. Further confirming that N_2O concentration in

the bucket silos were much higher than 5–ppm. In the spectrum of the silage gas, the saturation between 2200 cm^{-1} and 2400 cm^{-1} was due to the combined strong absorptions of CO_2 and N_2O. Fig. 3 – 5 shows the FTIR, fitted and residual spectra. The optical path length of the white cell was calibrated to 57.6m while the N_2O columns in the white cell along the optical path derived from the three spectral windows were $6.99 \times 10^{21} m^{-2}$, $6.69 \times 10^{21} m^{-2}$ and $7.18 \times 10^{21} m^{-2}$respectively. The converted N_2O concentrations were found to be 4.94 ppm, 4.91 ppm and 5.08 ppm respectively, corresponding to -1.2%, -1.8% and 1.6% different from the expected values of 5 –ppm. These confirms that N_2O can be accurately retrieved from FTIR spectra using LINEFIT program. Uncertainties caused by general spectroscopic error and experimental error were not accounted for as these contributes less than 10% to the error estimate for FTIR measurement (Smith *et al*, 2011).

Though Wang and Burries (1960) measured N_2O concentration in the farm silos using mass spectroscopy and reported N_2O varying around 10,000 to 43,500 ppm in the first 66 hours with its peak at about 54 hours after ensiling. This is many times greater than the N_2O concentration in the laboratory bucket silos measured in the present study. The differences in the two measurements could be because of introduced uncertainty in the mass spectroscopic measurement, differences in sampling locations and methods or the N_2O concentration between farm silos and bucket silos might be truly different.

6.0. Conclusion

The spectral resolution of FTIR spectroscopy at 1 cm^{-1} coupled with a long path white cell was used to analyze N_2O in a silage gas produce by corn silage prepared in a laboratory bucket silos. Absorption peak fingerprints of N_2O were identified in the FTIR spectra of the silage gas using both standard N_2O gas spectra and simulated spectra from the Infrared spectral database. N_2O concentrations retrieved from three spectral regions of the 5 – ppm N_2O spectrum were averaged $4.98 \pm 0.09\ ppm$. These confirms N_2O accurately retrieved from FTIR spectra using LINEFIT program.

References

Bacenetti, J. and Fusi, A. (2015). The environmental burdens of maize silage production: Influence of different ensiling techniques. *Anim. Feed Sci. Tech.* **204**, Pp: 88–98

Bell, A.J. (1972). *"Introductory Fourier Transform Spectroscopy",* Academic Press, New York.

Bergland, G.D. (1969). "A Guided Tour of the Fast Fourier Transform." *IEEE Spectrum,* Vol**. 6,** No.7, Pp: 41-52

Forester, P., Ramaswamy, V., Artaxo, P., Berntsen, T., Betts, R., Fahey, D.W., Haywood, J., Lean, J., Lowe, D.C., Myhre, G., Nganga, J., Prinn, R., Raga, G., Schulz, M. and Van Dorland, R. (2007). Changes in Atmospheric Constituents and in Radiative Forcing. *In: Climate Change 2007: The Physical Science Basis. Contribution of Working Group I to the Fourth Assessment Report of the Intergovernmental Panel on Climate Change* [Solomon, S., Qin, D., Manning, M., Chen, Z., Marquis, M., Averyt, K.B., Tignor, M. and Miller, H.L. (eds.)]. Cambridge University Press, Cambridge, United Kingdom and New York, NY, USA.

Hafner, S.D., Franco, R.B., Kung Jr., L., Rotz, C.A. and Mitloehner, F. (2014). Potassium Sorbate Reduces Production of Ethanol and 2 Esters in Corn Silage. *Journal of Dairy Sciences* , **97**, Pp: 7870 - 7878.

Hafner, S.D., Howard, C., Muck, R.E., Franco, R.B., Montes, F., Green, P.G., Mitloehner, F., Trabue, S.L. and Rotz, C.A. (2013). Emission of Volatile Organic Compounds from Silage: Compounds, Sources, and Implications. *Atmospheric Environment.* **77**, Pp: 827 - 839.

Harris, F.J. (1978). On the use of Windows for Harmonic Analysis with the Discrete Fourier Transform. *Proceedings of the IEEE*, **66** Pp: 172 - 204.

Hase, F. (2012). Improved Instrumental Line Shape Monitoring for the Ground-Based, High-Resolution FTIR Spectrometers of the Network for the Detection of Atmospheric Composition Change. Atmospheric Measurement Techniques, **5**, Pp: 603-610.

Hase, F., Blumenstock, T., and Paton-Walsh, C. (1999). Analysis of the instrumental line shape of high-resolution Fourier transform IR spectrometers with gas cell measurements and new retrieval software., Applied optics, **38**, Pp: 3417–3422.

Hase, F., Drouin, B.J., Roehl, C.M., Toon, G.C., Wennberg, P.O., Wunch, D., Blumenstock, T., Desmet, F., Feist, D.G., Heikkinen, P., De Maziere, M., Rettinger, M., Robinson, J., Schneider, M., Sherlock, V., Sussmann, R., Te, Y., Warneke, T. and Weinzierl, C. (2013). Calibration of Sealed HCl Cells Used for TCCON Instrumental Line Shape Monitoring. Atmospheric Measurement Techniques, **6**, Pp: 3527-3537.

Herres, W. (1984). *"Capillary GC-FTIR Analysis of Volatiles: HRGC-FTIR" In Proceedings.* Schreier, P. (eds), *"Analysis of Volatiles Methods, Application",* Walter de Gruyter & Co., Berlin. Pp: 183 – 217.

Herres, W. and Gronholz, J. (1984). "Understanding FT – IR data Processing. Part 1: data acquisition and Fourier transformation," *Comp. Appl. Lab.*, **2** Pp: 216 – 220.

IPCC (2007a). Annex I (glossary) to the fourth assessment report, Geneva.

IPCC (2007b). "Chapter 7: Couplings Between Changes in the Climate System and Biogeochemistry". IPCC WG1 AR4 Report. IPCC. 2007. Pp. FAQ 7.1.

IPCC (2009). *Meeting Report of the Expert Meeting on the Science of Alternative Metrics* ed G-K Plattner *et al* IPCC Working Group I Technical Support Unit, University of Bern, Bern, Switzerland.

Johnson, H.E., Merry, R.J., Davies, D.R., Kell, D.B., Theodorou, M.K. and Griffith, G.W. (2005). Vacuum Packing: A Model System for Laboratory-Scale Silage Fermentations. *Journal of Applied Microbiology*, **98**, Pp: 106 -113.

Linn, D.M. and Doran, J.W. (1984). Effect of Water-Filled Pore Space on Carbon Dioxide and Nitrous Oxide Production in Tilled and Nontilled Soils. *Soil Science Society of America Journal*, **48**, Pp: 1267 - 1272.

Liu, C., Yao, Z., Wang, K. and Zheng, X. (2014). Three -Year Measurements of Nitrous Oxide Emissions from Cotton and Wheat-Maize Rotational Cropping Systems. Atmospheric Environment, **96**, Pp: 201-208.

Mann, M. E. (2014). "Earth Will Cross the Climate Danger Threshold by 2036". Scientific American. Retrieved 30 August 2016.

Mertz, L. (1967). Auxiliary Computation for Fourier Spectrometry *Infrared Phys.* **7** Pp:17.

Mora, C. (2013). "The projected timing of climate departure from recent variability". Nature. 502 (7470), Pp: 183–187.

Myhre, G., Shindell, D., Bréon, F.-M., Collins, W., Fuglestvedt, J., Huang, J., Koch, D., Lamarque, J.-F., Lee, D., Mendoza, B., Nakajima, T., Robock, A., Stephens, G., Takemura, T. and Zhang, H. (2013). Anthropogenic and Natural Radiative Forcing. In: *Climate Change 2013: The Physical Science Basis. Contribution of Working Group I to the Fifth Assessment Report of the Intergovernmental Panel on Climate Change* [Stocker, T.F., Qin, D., Plattner, G.-K., Tignor, M., Allen, S.K., Boschung, J., Nauels, A., Xia, Y., Bex, V. and Midgley, P.M. (eds.)]. Cambridge University Press, Cambridge, United Kingdom and New York. NY, USA. Pp:659

Neal, W.M. and Becker, R.B. (1933). A Type of Laboratory Silo and Its Use with Crotalaria. *Journal of Agricultural Research*, **47**, Pp: 617- 625.

Ramaswamy, V., Boucher, O., Haigh, J. and Hauglustaine, H. (2001). Radiative forcing of climate change. In: *Climate Change 2001: The Scientific Basis. Contribution of Working Group I to the Third Assessment Report of the Intergovernmental Panel on Climate Change* [Houghton, J.T., Ding, Y.,Griggs, D.J. and Noguer, M (eds.)]. Cambridge University Press, Cambridge, United Kingdom and New York, NY, USA, Pp: 349 – 416.

Reid, W.S., Turnbull, J.E., Sabourin, H.M. and Ihnat, M. (1984) Silo Gas: Production and detection. *Canadian Agricultural Engineering*, **25**, Pp:197-207.

Smith, T.E.L., Wooster, M.J., Tattaris, M. and Griffith, D.W.T. (2011). Absolute Accuracy and Sensitivity Analysis of OP-FTIR Retrievals of CO_2, CH_4 and CO over Concentrations Representative of “Clean Air” and “Polluted Plumes”. Atmospheric Measurement Techniques, **4**, Pp: 97-116.

Van Groenigen, J.W., Kasper, G.J., Velthof, G.L., van den Pol-van Dasselaar, A. and Kuikman, P.J. (2004). Nitrous Oxide Emissions from Silage Maize Fields under Different Mineral Nitrogen Fertilizer and Slurry Applications. Plant and Soil, **263**, Pp: 101-111.

Wang, L.C. and Burries, R.H. (1960). Mass Spectrometric Study of Nitrogenous Gases Produced by Silage. Agricultural and Food Chemistry, 8, Pp: 239 - 242.

Weinberg, Z. G. and Ashbell, G. (2003). Engineering aspects of ensiling. *Biochem. Eng. J.* **13**, Pp:181–188

Weinberg, Z. G. and Ashbell, G. (2003). Engineering aspects of ensiling. *Biochem. Eng. J.* **13**, Pp: 181–188.

Wunch, D., Taylor, J.R., Bernath, D. F. P., Drummond, J.R., Midwinter, C., Strong, K. and Walker, K.A. (2007). Simultaneous Ground-Based Observations of O_3, HCl, N_2O, and CH_4 over Toronto, Canada by Three Fourier Transform Spectrometers with Different Resolutions. *Atmospheric Chemistry and Physics*, **7**, Pp: 1275-1292.